Alexandria Engineering Journal (2022) 61, 3201–3214

HOSTED BY

ELSEVIER

Alexandria University

Alexandria Engineering Journal

www.elsevier.com/locate/aej
www.sciencedirect.com

Using nanomaterial to minimize the local scour downstream of sluice gate

M.M. Ibrahim [a], A. Helmy [b], M.A. Alafrawi [c], A.N. El-Hazek [a]

[a] Faculty of Engineering at Shoubra, Cairo, Benha University, Egypt
[b] Faculty of Engineering, Al-Azhar University, Cairo, Egypt
[c] Pyramids Higher Institute for Engineering and Technology, 6th October City, Egypt

Received 16 April 2021; revised 5 June 2021; accepted 14 August 2021
Available online 26 August 2021

KEYWORDS

Sluice gate;
Nanomaterial;
Silica fume;
Scouring;
Silting;
Dry-mix;
Wet-mix

Abstract Prediction of scour depths is an important aspect related to the overall stability of hydraulic structures. In this research, small-scale laboratory experiments were carried out to explore the effectiveness of mixing different percentages of Nanomaterial (Silica fume) to non-cohesive (alluvial) movable bed soil to develop mixture of bed material with significant characteristics to minimize the local scour caused by high-velocity jets downstream of a sluice gate. The experiments were executed employing 9 jet Froude numbers ranged from 1.88 to 2.81 associated with 3 heights for gate opening, and 3 tailwater depths. The bed material has 5 different percentages of Silica fume mixed by weight and 2 types of mixing with and without water were used. Ninety-nine experiments were conducted, out of which 9 experiments were done using fine sand as a bed material for the referenced cases. Graphical relationships were presented for maximum scouring and silting depths for different hydraulic conditions and bed materials. This research demonstrated that the type of mix (dry-mix or wet-mix) had a significant influence on the geometry of scouring and silting for the same flow conditions and the mixed percentage ratio of Silica fume. For dry-mix, the scouring and silting depths increased as the percentage ratio of Silica fume increased. While for wet-mix, the scouring and silting depths decreased as the percentage ratio of Silica fume increased. Also, the wet-mix effectively reduced the local scour volumes by 34.65% and 83.05% and decreased the silting volumes by 33.35% and 89.42% according to the percentage of Silica fume. Using a bed mixture of 8% Silica fume wet-mix showed 83.05% and 89.42% decrease in scouring and silting volumes, respectively, compared to pure fine sand bed material. From practical and financial aspects, the presented composition of bed material can effectively replace the smooth apron or at least decrease its length to reduce the construction cost. The obtained results present an untraditional technique for local scour protection downstream hydraulic structures.

Peer review under responsibility of Faculty of Engineering, Alexandria University.

https://doi.org/10.1016/j.aej.2021.08.035
1110-0168

Nomenclature

b_o	**Gate opening height [m]**	M_r	The mixture ratio
B	Flume width [m]	R_e	Reynolds number
d_{50}	Median sediment diameter [m]	S_s	Specific gravity of sediment
d_{90}	Particle size for which 90% are finer by weight [m]	u_c^*	Critical bed-shear velocity [m/s]
d_{95}	Particle size for which 95% are finer by weight [m]	V_j	Jet velocity [m/s]
d_s	Maximum equilibrium scour depth [m]	V_o	Mean jet velocity at the efflux section [m/s]
F_r	Flow Froude number	V_{abs}	The mixture absolute volume [Liter]
F_{rj}	Jet Froude number	W_s	Weight of fine sand in bed soil [kg]
Fr_{dj}	jet densimetric Froude number	W_{si}	Weight of Silica fume in bed soil [kg]
$Fr_{dj\ (95)}$	jet densimetric Froude number based on d_{95}	W_w	Weight of water in bed soil [kg]
F_{ro}	Sediment densimetric Froude number	y_j	Jet thickness (vertical dimension) [m]
G_s	The specific weight of fine sand	y_s	Local scour depth [m]
G_{si}	The specific weight of Silica fume	y_t	Tailwater depth [m]
g	Gravitational acceleration [m/s^2]	ρ	Fluid density [kg/m^3]
H_{up}	Upstream water depth [m]	ρ_s	Sediment density [kg/m^3]
K_D	Effect of sediment size	υ	Kinematic viscosity of the fluid [m^2/s]
K_L	Effect of apron length	σ_g	The standard deviation of the particle size distribution
K_t	Effect of tailwater depth	θ	adverse slope on stilling basin
K_σ	Effect of sediment gradation	φ	Angle of repose
k_e	Roughness height of the apron [m]		
L	Apron length [m]		

1. Introduction

Water released at high flow velocity underneath hydraulic structures, such as sluice gates has a significant amount of potential energy, that causes stability problems to the downstream bed material such as scour process. Scour can make remarkable damage to the structural elements of the hydraulics structures or even sudden structure failure leading to massive economic losses. Thusly, investigating the local scour downstream hydraulic structure is an important phenomenon that keep researchers' attention for many decades. Studying the downstream local scour process is a very complex problem that is functional in numerous variables related to the heterogeneity of the bed soil and the flow conditions that produce the erosive action [1]. For a typical scouring process, there are three observable stages of scouring which are initial, development, and equilibrium stages. The initial stage is characterized by a rapid rate of scouring, the development or erosion stage has a relatively slower rate of scouring, and an equilibrium stage where the changes in the scour depth after a long scouring time are unnoticed [2]. Many experiments have been conducted to study the scouring action associated with 2-D jets that included the studies by Tarapore [3], Basmaci [4], Rajaratnam [5], Ali and Lim [6], Valentin [7], Altinbilek and Basmaci [8], Breusers and Raudkivi [9], Chatterjee et al., [10], Aderibigbe and Rajaratnam [11], Melville and Lim [12], Gamal [13], Melville [14], Chen and Siow [15].

With the improvement of soft computing techniques, recently many researchers used numerical models to predict the scour characteristics downstream sluice gate; such as Najafzadeh [16], Najafzadeh et al., [17], Yousif et al., [18], Ahmad et al., [19], Mehmet and Cimen [20], Hamid et al., [21], and Hamidreza et al., [22].

To protect the structures from failure by the scouring action, a typical engineering solution is to construct a solid apron downstream of the structures to minimize the effect of erosion from the structures. The scour downstream sluice gate with an apron was studied by Choudhary [23], Verma and Arun [24], Iwagaki et al., [25], Hassan and Narayanan [26], Li [27], Lim and Yu [28], Luis [29].

Different techniques to reduce the local scour downstream sluice gates have been employed. The baffle blocks and end sill with different shapes and dimensions installed to the stilling basin were used. Many studies were done; such as Ibrahim [30], Alireza [31], Valinia et al., [32], Saleh [33], Mohsen et al., [34].

Javad and Hossein [35] conducted experiments in a wide range of adverse slopes on stilling basin, $0 \leq \tan\theta \leq 0.156$; the size of bed material, $0.023 \leq \frac{d_{50}}{b_o} \leq 0.127$. The study concluded that the adverse stilling basin decreased the scour downstream sluice gate for different flow conditions. Yehia et al., [36] carried out 57 runs to explore the influence of pendulum sill downstream sluice gate. Different gate openings and discharges were used. It was found that the pendulum sill decreased the scour provided that it is located in the first half of the hydraulic jump. Ibrahim, [37] experimentally tested the influence of angled submerged vans installed in the apron on the scour downstream a sluice gate. Three vans angles were used 45°, 90°, and 135°. The runs were conducted under 3 discharges and 3 tailwater depths. The study was carried out under the size of bed material, $0.027 \leq \frac{d_{50}}{b_o} \leq 0.103$; jet Froude number $1.5 \leq F_{rj} \leq 4.1$. It was concluded that using angled submerged vanes of 45° pointed against the flow direction showed a noticeable reduction in scour depth.

The Computational Fluid Dynamic, CFD are widely used to simulate the flow and bed configurations downstream of hydraulic structure considering unconventional techniques for scour protection. Akbar [38] explored the effectiveness of air injection after the formation of the hydraulic jump on the scour reduction downstream of a stilling basin. The study showed a significant reduction in turbulent kinetic energy due to the presence of the air bubbles which is the main reason for reducing the scour. Imanian and Mohammadian [39] studied the hydrodynamic field under high head ratio conditions passed over an ogee-crested spillway. It was found that with increasing the hydraulic head, up to seven times that of the design head, the flow separation zone showed linear performance. Yang et al., [40] investigated the influence of the air–water momentum exchange in the two-phase Two-Fluid Model. The study concluded that the models were evaluated for calculations of entrained air characteristics of a flowing mixture with an approach velocity of 14.3 m/s. Samadi et al., [41] developed a new soft computing tool for estimating the equilibrium scour depth downstream free overfall spillways. Statistical indicators demonstrated that the developed model showed a good performance and presented competitive results for the prediction of this phenomenon. Sammen et al., [42] employed a novel optimization algorithm, namely, Harris hawks optimization (HHO), to enhance the performance of an artificial neural network (ANN) to predict scour depth downstream of the ski-jump spillway. The graphical inspection displayed better accuracy of the ANN-HHO model compared to the other models for the prediction of scour depth downstream the ski-jump spillway.

The technique of air injection was also experimentally examined by Ted et al., [43]. They investigated in a rectangular flume the feasibility of vertical air injection for scouring reduction downstream spillway. The outcomes revealed that the scour depth was decreased by 59% and 37% near and far from the structure, respectively provided that the airflow to water velocity ratio was 251. Gamal et al., [44] used 5 rows of floor water jets installed and arranged symmetrically in the stilling basin to investigate their effects on decreasing the dimensions of the scour formed downstream radial gate. A wide range of hydraulic conditions was used including 3 discharges and 3 tailwater depths. The study showed that the floor water jets installed and arranged in the stilling basin effectively decreased the downstream scour depth. Khalifehei et al., [45] employed an experimental model to examine the local scour at the end of flip bucket energy dissipaters under various flow rates and tailwater depths. The results showed that the maximum depth of scouring and its distance from the structure increased by increasing the discharge. Khalifehei et al., [46] experimentally investigated the effectiveness of A-Jack concrete blocks for riverbeds protection downstream hydraulic structure. The study demonstrated that the A- Jack concrete blocks showed good performance in decreasing the scour and silting ranges and increasing the energy dissipation.

Amir et al., [47] carried out experimental tests on Nanostructured materials in a rectangular flume to investigate their effect on scouring reduction of alluvial beds downstream stepped spillway. The results showed that these additives decreased the scour depth and length by 41% and 38%, respectively, also controlling the scour mechanism specifically in flood charges.

From reviewing the previous researches related to minimizing the local scour downstream hydraulic structures, it is noticed that they used limited techniques based on the implementation of stilling basin and introducing some modifications to increase its efficiency. Very few studies considered to develop bed material with special characteristics for scour protection with special attention to replace the stilling basin or at least shorten its length. Thus, the current study is initiated to continue studies considering the novel technique for scouring protection downstream sluice gate by adding Silica fume as a Nanomaterial mixed with fine sand. The used Silica fume has a high content of amorphous silicon dioxide, consists of very fine spherical particles, and is collected from the gases escaping from the furnaces. Different percentages Silica fume; 1, 2, 4, 6 and 8% are mixed in dry and wet conditions to the fine sand to form a composite of bed material with resistance to the scour by jet flow action downstream of sluice gate under different flow conditions considering three gate opening heights of b_o = 1, 1.25, and 1.5 cm and three tailwater depths of y_t = 14, 15, and 16 cm.

2. Dimensional considerations

Several parameters affect jet scour in an alluvial bed, which are listed as follows:

$$d_s = f_1(\upsilon, \rho, \rho_s, d_{50}, \sigma_g, B, H_{up}, y_t, k_e, V_o, L, b_o, g, W_{si}, W_s) \quad (1)$$

Where d_s = maximum equilibrium scour depth, (m); υ = kinematic viscosity of fluid, (m^2/s); ρ = fluid density, (m^2/s); ρ_s = sediment density, (m^2/s), d_{50} = median sediment diameter, (m); σ_g = standard deviation of particle size distribution, B = flume width, (m); H_{up} = upstream water depth, (m); y_t = tailwater depth, (m); k_e = roughness height of the apron, (m); V_o = mean jet velocity at the efflux section, (m/s); L = apron length, (m); b_o = gate opening height, (m); g = gravitational acceleration, (m/s^2); W_s = weight of fine sand, (kg); W_{si} = weight of Silica fume, (kg).

Dividing Eq. (1) by y_t, introducing R_e is the Reynolds number $= \frac{V_o b_o}{\upsilon}$, F_r is the flow Froude number $= \frac{V_0}{\sqrt{g d_{50}}}$, and S_S is the specific gravity of sediment $= \frac{\rho_s}{\rho}$, Eq. (1) becomes:

$$\frac{d_s}{y_t} = f_2\left(R_e, \frac{d_{50}}{y_t}, \frac{k_e}{y_t}, S_s, \sigma_g, \frac{H_{up}}{y_t}, F_r, \frac{L}{y_t}, \frac{B}{y_t}, W_{si}, W_s\right) \quad (2)$$

Some terms in Eq. (2) may be neglected or combined. First, the ratio between the Silica fume and fine sand weights W_{si}/W_s can be combined to form the mixture ratio, M_r. Second, the specific gravity of sediment, S_s and the flow Froude number, F_r can be combined to form sediment densimetric Froude number, $F_o = \frac{V_0}{\sqrt{(S_s-1) g d_{50}}}$. Third, the jet velocity is usually relatively high, therefore the corresponding Reynolds number, R_e may be neglected. This mean the viscosity influence on the jet hydraulics and its scouring is insignificant. Forth, the apron roughness parameter, k_e/y_t may be also neglected because no apron is used in the current study. Moreover, B, d_{50}, H_{up} and σ_g are kept constants therefore they are ignored. Hence, Eq. (2) becomes as follows:

$$\frac{d_s}{y_t} = f_3\left(\frac{d_{50}}{y_t}, \frac{H_{up}}{y_t}, F_o, M_r\right) \quad (3)$$

3. Methods and materials

3.1. Scheme of experimentation

The experimental studies were carried out in the hydraulic laboratory flume of the Civil Engineering Department, Faculty of Engineering, Al-Azhar University, Egypt.

The model was tested in a recirculating flume of 4 m long, 0.30 m wide, and 0.50 m deep as shown in Fig. 1. The side walls are clear polycarbonate to allow visual monitoring for the water surface and the bed profile, also to avoid deformations by the action of water. The floor is fixed on a steel truss. The flume has head and tail tanks. Water is pumped to the head tank from the ground sump. Two pipes with a 4.2-inch diameter with a control valve were used to recirculate the flow. Tailgate is placed downstream of the channel to control the tailwater depth. Rectangular calibrated sharp-crested weir was fixed downstream the gravel box to measure the discharge. The weir is 0.25 m in width and sharp edges made of copper. The flow discharges were measured by the crested weir and double-checked by a flowmeter of ± 1% accuracy.

For measuring water and bed levels at different points of the channel, an x–y carriage was supported on the channel sides and it could be moved along the channel length. A point gauge with an accuracy of 0.1 mm was fitted on the carriage to measure both water and bed levels along the channel length and across the channel width. Also, a levelling device was used as a double check for the hydraulic parameters and bed profile measurements.

The bed material was a mixture of fine sand and Silica fume mixed by weight to simulate the movable bed. The used fine sand had grain median size d_{50} = 0.7 mm with standard deviation σ_g = 1.3. The used Silica fume has physical properties of 350 kg/m^3 bulk density and 16.7 m^2/gm specific surface area. The used sluice gate model was 0.001 m thick, 0.4 m high, 0.3 m wide, and was made of steel.

3.2. Difficulties, challenges, and proposed solutions

The carried experimental tests has some difficulties and challenges that should be adopted before and during the laboratorial experiments. Before the experimental process, the selection of Nanomaterial was a challenge. Many of alternatives were tried, e.g. clay, and Nano-clay Montmorillonite, and Silica fume. The Silica fume was adopted in the experiments as it has the following advantages: it formed homogeneous mixture with the fine sand with and without the presence of water; it was easily obtainable from the furnaces and material markets; finally it has relatively cheaper price compared to other Nanomaterial alternatives. Also, it was recommended to be used in other studies, e.g. Amir et al., [47].

The adaptation of water quantity in the bed mixture in case of wet-mix was also challenge, where many alternatives were suggested, e.g. the absolute volume, the empirical, the trial, the optimum unit weight, and the surface area methods. The absolute volume method was applicable and gave accurate results for the instance of the used very fine particles (i.e. the Nanomaterial) has relatively high bulk density, which is introduced in the current experimental work. Moreover, due to its simplicity in application, the quantity of water used in the wet-mix was determined using the absolute volume method which is also widely used for concrete design mixture.

The absolute volume method assumed that the absolute volume of the mixture is the sum of the absolute volumes of

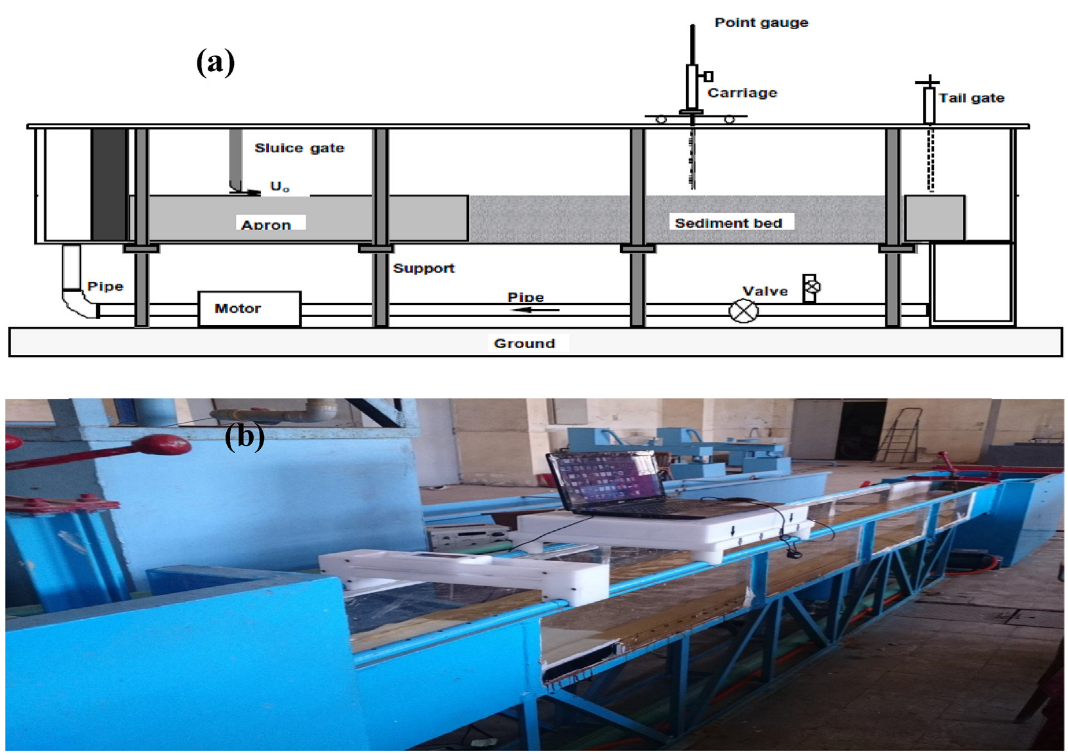

Fig. 1 The used flume: (a) layout; (b) photo.

the component materials, i.e. the absolute volumes of sand, Silica fume, and water as follows:

$$V_{abs} = \frac{W_s}{G_s} + \frac{W_{si}}{G_{si}} + \frac{W_w}{1} = 1000 litres \quad (4)$$

Where V_{abs} = the mixture absolute volume, W_s = the weight of fine sand in the mixture, W_{si} = the weight of Silica fume in the mixture which is presented in terms of fine sand weight, W_w = the required weight of added water in the mixture, G_s = the specific weight of fine sand = 2.65, G_{si} = the specific weight of Silica fume = 2.2.

Regarding the laboratorial challenges, they were started form the flume selection. The used flume was adopted according to the available facilities regarding dimensions, pump capacity, and feeding systems to cover the proposed scenarios. To confirm the bed material was accurately levelled and fitted in its place, a sharp long stick was used and levels were also double checked using a levelling device at different locations. The process of bed levelling was done for each test before the flume filling. A screen stone box filled with large gravel was employed at the flume entrance to develop a uniform flow and scatter the water turbulence. Back water feeding was slowly initiated for flume filling to avoid any bed configurations due to upstream water feeding before the run time starts. Finally, the bed profile measurements after each run were also a challenge. The measurements were taken twice times utilizing point gauges and levelling device, where the mean values were introduced at 126 locations covered the bed material.

3.3. Justifications of parameters assumptions

The current experimental work has some parameter assumptions as a preliminary assessment which was obtained after few trial tests. Considering the amount of Silica fume in the mixture, many percentages were tried with the pure sand. The adopted percentages were ranged between 1% and 8%. The alternatives less than 1% introduced unremarkable changes in bed material compared to the pure fine sand in case of wet-mix. However, the Silica fume more than 8% were noticeably segregated from sand in case of dry-mix.

Nine jet Froude numbers presented in Table 2 were tested according to the gate opening and the tailwater depths presented in the test program in Table 1. The adopted jet Froude numbers were ranged between 1.88 and 2.81. The alternatives less than 1.88 gave insignificant bed disturbance in the case of 1% Silica fume wet-mix. However, the values more than 2.81 led to complete movement of the bed material especially in the case of 8% Silica fume dry-mix.

The adopted gate openings were between 1 and 1.5 cm, however the tested tailwater depths were between 14 and 16 cm. The adopted ranges were according to the available facilities and the study domain. In addition, the recorded configurations in bed material under different percentages of Silica fume. Where, gate openings less than 1 cm demonstrated complete removal for bed material in the case of the tailwater depth was 14 cm. On the contrary, no appreciable changed were recorded for tests of gate openings more than 1.5 cm and tailwater depths more than 16 cm.

3.4. Experimental procedure

The test procedure consisted of the following steps:

1) The bed material was fitted in its place and accurately leveled to cover length, width, and depth of 100 cm, 30 cm, and 6.5 cm, respectively.
2) The sluice gate was accurately placed in its location and completely closed.
3) Backwater feeding was slowly started using a submerged pump not to disturb the bed levels.
4) The main pump was turned on and the upstream flow is in progress up to the desired upstream water depth (H_{up} = 22 cm).
5) The desired gate opening was set, where three different gate openings were studied (b_o = 1.00, 1.25, and 1.50 cm).
6) Simultaneously, the tailgate was tilted to adjust the tailwater depth, where three depths of tailwater were investigated (y_t = 14, 15, and 16 cm).
7) The run time duration is started, the hydraulic measurements are recorded after 360 minimum, the position of the hydraulic jump is adjusted, the flow rate and the water surface profile are recorded.
8) The main pump was switched off and the tailgate was completely opened to drain the water.
9) After complete drainage, the measurements of the bed profile are started and the topographical bed characteristics are recorded.

Three sets of experiments with 99 experimental runs were conducted and categorized into 3 sets according to the characteristics of bed material and conditions of mixture. For each set, 9 identical hydraulic conditions were applied using 3 gate openings, b_o and 3 tailwater depths, y_t. Set (A), presented the referenced case and consisted of 9 runs in which the bed material was pure fine sand where no Silica fume was introduced. Set (B), consisted of 45 runs in which 5 percentages of Silica fume were mixed in dry conditions to the fine sand. Set (C), used similar hydraulic conditions and percentages of Silica fume of set (B) but the Silica fume was mixed to the fine sand in the presence of determined quantity of water. The primary details were summarized in Table 1.

The bed materials were stored in a suitable place on the site away from the moisture effect. For emphasizing the mixing methodology for fine sand and Silica fume, the following steps were used:

Table 1 Primary details of the experiments.

Series	b_o (cm)	y_t (cm)	% Silica fume	Type of mixture
Set A (9 runs)	1, 1.25, 1.5	14, 15, 16	N/A	N/A
Set B (45 runs)	1, 1.25, 1.5	14, 15, 16	1, 2, 4, 6, 8	Dry
Set C (45 runs)	1, 1.25, 1.5	14, 15, 16	1, 2, 4, 6, 8	Wet

1) The desired percentage was determined by weight (e.g., if 10 gm Silica fume was mixed to 1000 gm of fine sand, that meant a mixture of 1% Silica fume).
2) The bed materials were mixed by hand using a shovel.
3) The mixing process was done in a dry wooden box three times until the color of the mixture became homogeneous.
4) In the case of the wet-mix, water was added gradually to achieve the required amount for mixing. Stirring and mixing were continued three times until the color and consistency of the mixture became homogeneous.

3.5. Run duration

To determine the run duration where the maximum scour depth was recorded, Fig. 2 is plotted. The figure presents the centerline bed profile recorded after different run durations ranged from 30 min up to 480 min. The runs were carried out on the pure fine sand bed material. The gate opening was 1 cm, and the tailwater depth was 14 cm. The figure demonstrates that as the time increases, the rate of changes in bed profile would decrease and eventually approached zero as the equilibrium scour hole has been reached. As seen in Fig. 2, approximately the maximum scour depth is achieved after 360 min as an equilibrium state of scouring has been reached, where the more increase in time leads to insignificant changes in bed profile. Hence, each test is run for 360 min, which is sufficient enough for all tests.

From figure investigations and the visual observations during the experimental runs, it is noticed that the mechanism of the scouring process has three phases. In the digging phase, when the jet is attached to the bed a lot of particles are transported. Then the jet starts to rise towards the horizontal position. Finally, by the time all the sediment deposits are back in the scour hole mid-section (the filling phase). These findings agree with Lim and Yu [2]. The figure also shows the angles of repose (φ) for the scour and sediment processes that are around 74.91° and 22.13°, respectively, regardless of the run time duration. Hence, the scour hole characteristics are underlined compared to the sedimentation. These findings agree with Lim and Yu [28].

4. Framework for analysis

The test program was carried out by utilizing 3 tailwater depths, 14, 15, and 16 cm, 3 gate openings, 1, 1.25, and 1.5 cm, using 6 types of bed material 0, 1, 2, 4, 6, and 8% of Silica fume. The tests were carried out for $\sigma_g = 1.3$ and a wide range of $D_{50}/y_j = 0.046$–0.07.

Regarding the jet Froude number, F_{rj}, it is varied according to the gate openings and the tailwater depths as tabulated in Table 2. The table shows that the F_{rj} increases by the increase of b_o for constant y_t. That is reasoned by under fixed upstream and downstream water depths, whenever the gate opening, b_o increases the more flow is released underneath the sluice gate at higher jet velocities and as a result, the jet Froude number, F_{rj} increases.

Emphasizing the tailwater depth, y_t, it is noticed that the jet Froude number decreases by the increase of the tailwater depth for fixed gate opening. That is illustrated as the difference between the upstream and the downstream water heads decreases, the released discharge is reduced. Consequently, the jet velocity and the associated jet Froude number are decreased.

4.1. Calibration of experimental measurements

For model validation, the local scour equations downstream of the sluice gate presented by [7–12] were used. These equations were accurately selected because their range of parameters covered the domain of the current study. Table 3 summarizes the equations used in the calibration process. The calculated and measured d_s/y_t were for the bed material used in the referenced case (i.e. the case of fine sand with 0% Silica fume). The comparison outcomes are presented in Fig. 3.

The figure indicates that around 79% of the data are within the ±20% error band and around 91% are within the ±30%

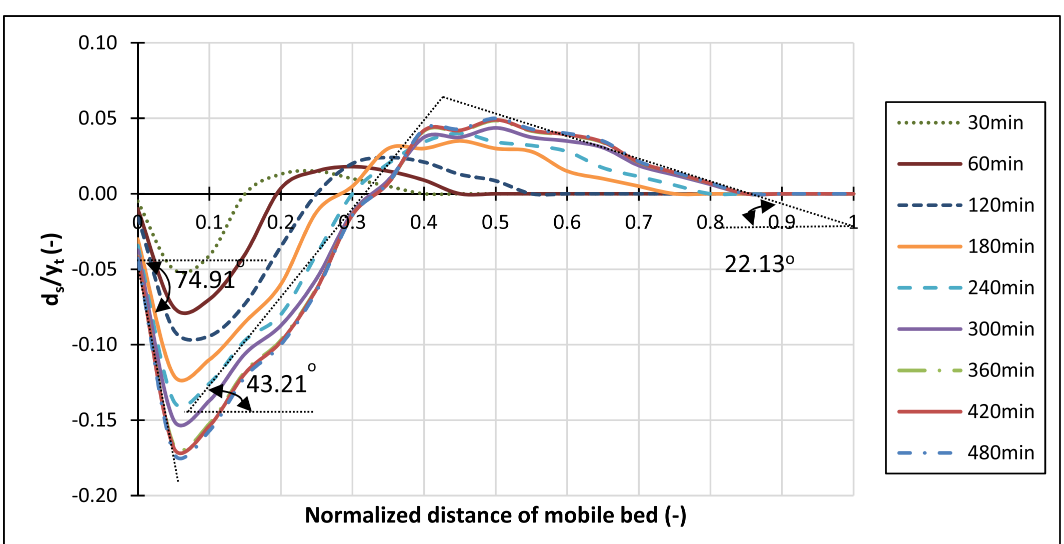

Fig. 2 The centerline bed profile for different run durations.

Table 2 Range of jet Froude number.

b_o (cm)	F_{rj} (-)		
	y_t (cm)		
	14	**15**	**16**
1.00	2.17	2.03	1.88
1.25	2.43	2.28	2.11
1.50	2.81	2.63	2.43

error band. Consequently, the experimental data for the referenced case are acceptable compared to the equations collected from the previous studies. At that moment, the model is validation.

4.2. Model runs

The scenarios were selected to characterize the influence of adding different percentages of Silica fume to fine sand and mixing the materials with and without water to develop a mixture with protective characteristics against the local scour downstream of the sluice gate under various flow conditions.

A designed dense mesh comprised of 126 measuring points distributed in 6 lines to cover the flume width and crossed by 21 sections to cover the total length along with the bed material. The spacing between lines were 0.025, 0.050, 0.150, 0.200, 0.250, and 0.275 m measured from flume sidewall to cover the total width of bed material. However, the sections were 0.05 m intervals and started directly by the beginning of the bed material (i.e. Sec. 1) and ended after 1 m (i.e. Sec. 21) to cover the total length of bed material. The mesh is dense enough to give sufficient discretization of the bed profile with high accuracy.

5. Results and discussions

5.1. Effect of Silica fume

To explore the influence of adding Silica fume to bed material besides the type of mixing to motivate and strengthening the fine sand to minimize the local scour downstream of the sluice gate, Figs. 4 and 5 are presented. The figures are plotted under constant jet Froude number $F_{rj} = 2.17$ which is associated to flow underneath gate opening $b_o = 1$ cm and tailwater depth $y_t = 14$ cm, respectively.

Fig. 4 shows the bed topography presented in dimensionless terms of d_s/y_t for 3 different types of bed materials; 0% Silica fume, 8% dry-mix, and 8% wet-mix. The figure demonstrates that adding the Silica fume to the fine sand significantly decreases the scour depth in the case of wet-mix. However, using the same percentage of Silica fume dry-mix indicates noticeable increase in the scour depth compared to the referenced case of the fine sand with 0% Silica fume. The reasons behind that are illustrated in the following sub-section.

The obtained scouring and silting depths along with the bed profile are plotted for different percentages of Silica fume for the dry-mix and the wet-mix in Fig. 5.

Combining the findings of Fig. 2 regarding the angles of repose for the scour and sediment processes and Fig. 5 emphasizing the geometry of scour hole, it is remarked that the upstream slope of scour hole is steeper than the downstream one. That is because the sediment grains initiated to move when the combined lift and drag forces produced by the flow become significant enough to counteract the gravity and frictional forces that stabilize the grains in place. Then after a distance, the particles lose their energy and start to deposit.

From Fig. 5 (a) concerning the dry-mix, it is found that the percentage of 8% of Silica fume is associated with maximum scouring and silting depths. While the referenced case of 0% Silica fume shows the minimum scouring and silting depths. Consequently, it is concluded that the turbulences in the bed profile increases as the percentage of Silica fume increase in case of dry-mix. That is because in the case of dry-mix when the flow starts, the particles of Silica fume immigrate their places in the mixture and segregate from the fine sand due to the lightweight and small particle size of Silica fume. That means the more increase in the percentage of Silica fume in the mixture is associated with more increase in bed turbulences in terms of scouring and silting. Fig. 5 (a) shows that the maximum scouring and silting depths increased by 114.1% and

Table 3 Scour equations used in the validation process.

Reference	Equation	Range of parameters		
		F_{rj}	D_{50}/y_j	σ_g
Valentin, [7]	$log\left(\frac{y_s}{y_j}\right) = \frac{Fr_j-2}{4.7} - log\left(\frac{D_{90}}{y_j}\right)$ where y_s = local scour depth, D_{90} = particle size for which 90% are finer by weight, F_{rj} = jet Froude number = $\frac{V_j}{\sqrt{gy_j}}$, V_j = jet velocity, and y_j = jet thickness (vertical dimension)	1.3–6.5	0.03–0.44	1.1–1.3
Altinbilek and Basmaci, [8]	$\frac{y_s}{y_j} = \left(\frac{y_j}{D_{50}} tan\varnothing\right)^{0.5} (Fr_{dj})^{1.5}$ D_{50} = median particle size, φ = angle of repose, Fr_{dj} = jet densimetric Froude number = $\frac{V_j}{\sqrt{(S_s-1)gD_{50}}}$, and S_S = specific gravity of sediment	1.6–9.9	0.04–1.05	N/A
Breusers and Raudkivi, [9]	$\frac{y_s}{y_j} = 0.008\left(\frac{y_j}{u_{*c}}\right)^2$ where u_{*c} = critical bed-shear velocity	1.8–10.5	0.02–0.50	1.1–3.9
Chatterjee et al., [10]	$\frac{y_s}{y_j} = 0.775Fr_j$	1.0–5.5	0.02–0.14	1.2–1.4
Aderibigbe and Rajaratnam, [11]	$\frac{y_s}{y_j} = 3.35Fr_{dj(95)} - 6.11$ where $Fr_{dj(95)}$ = jet densimetric Froude number based on D_{95}	1.2–21.5	0.05–1.35	1.3–3.1
Melville and Lim, [12]	$\frac{y_s}{y_j} = 3Fr_jK_DK_tK_\sigma K_L$ where K_D = the effect of sediment size, K_t = the effect of tailwater depth, K_σ = the effect of sediment gradation, and K_L = the effect of apron length.	1.0–12	0.003–1.38	≤1.5

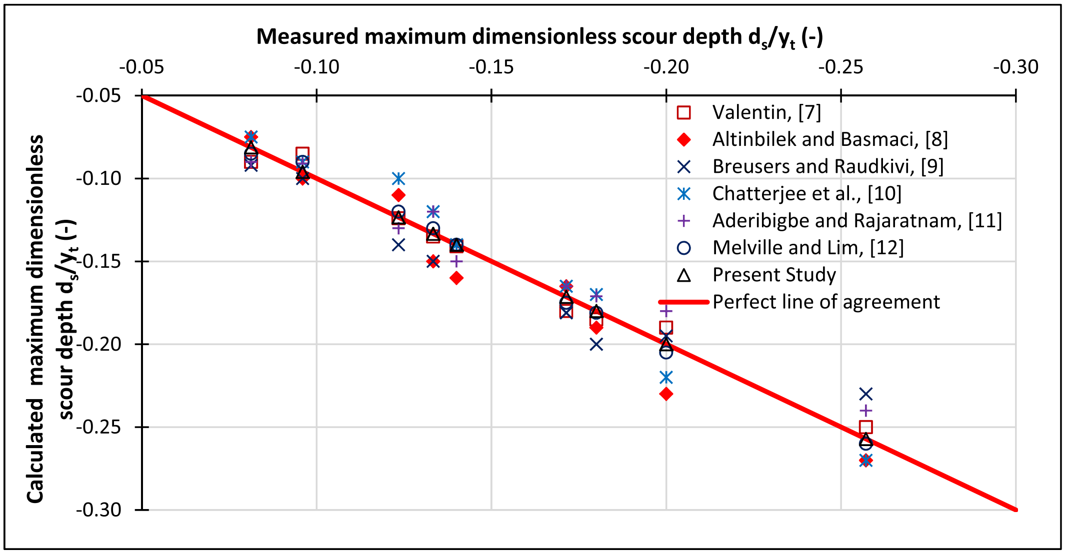

Fig. 3 Comparing measured and calculated dimensionless maximum scour depths.

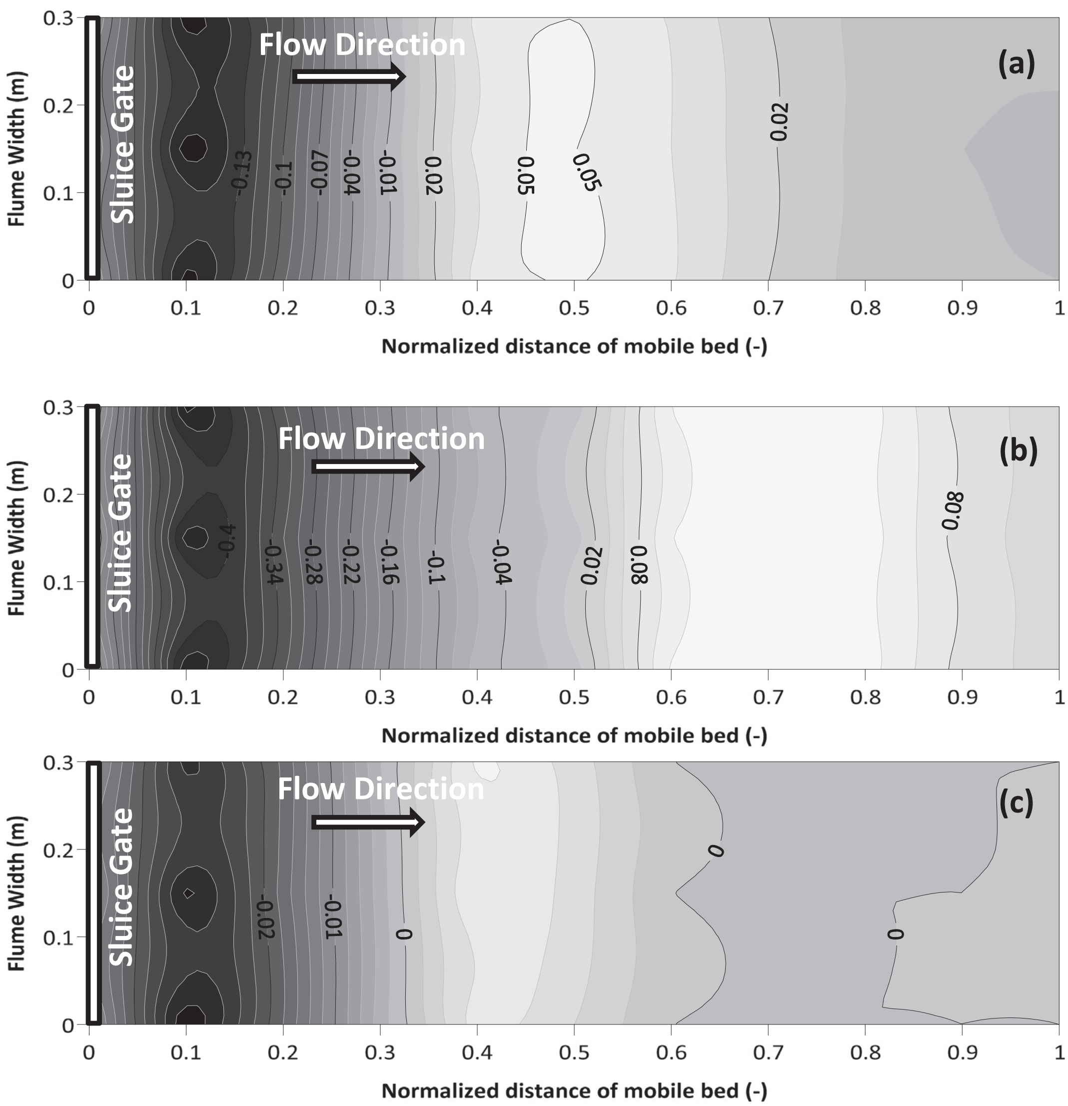

Fig. 4 Contour map of the obtained scouring depths: (a) 0% Silica fume, (b) 8% Silica fume Dry-Mix, and (c) 8% Silica fume Wet-Mix.

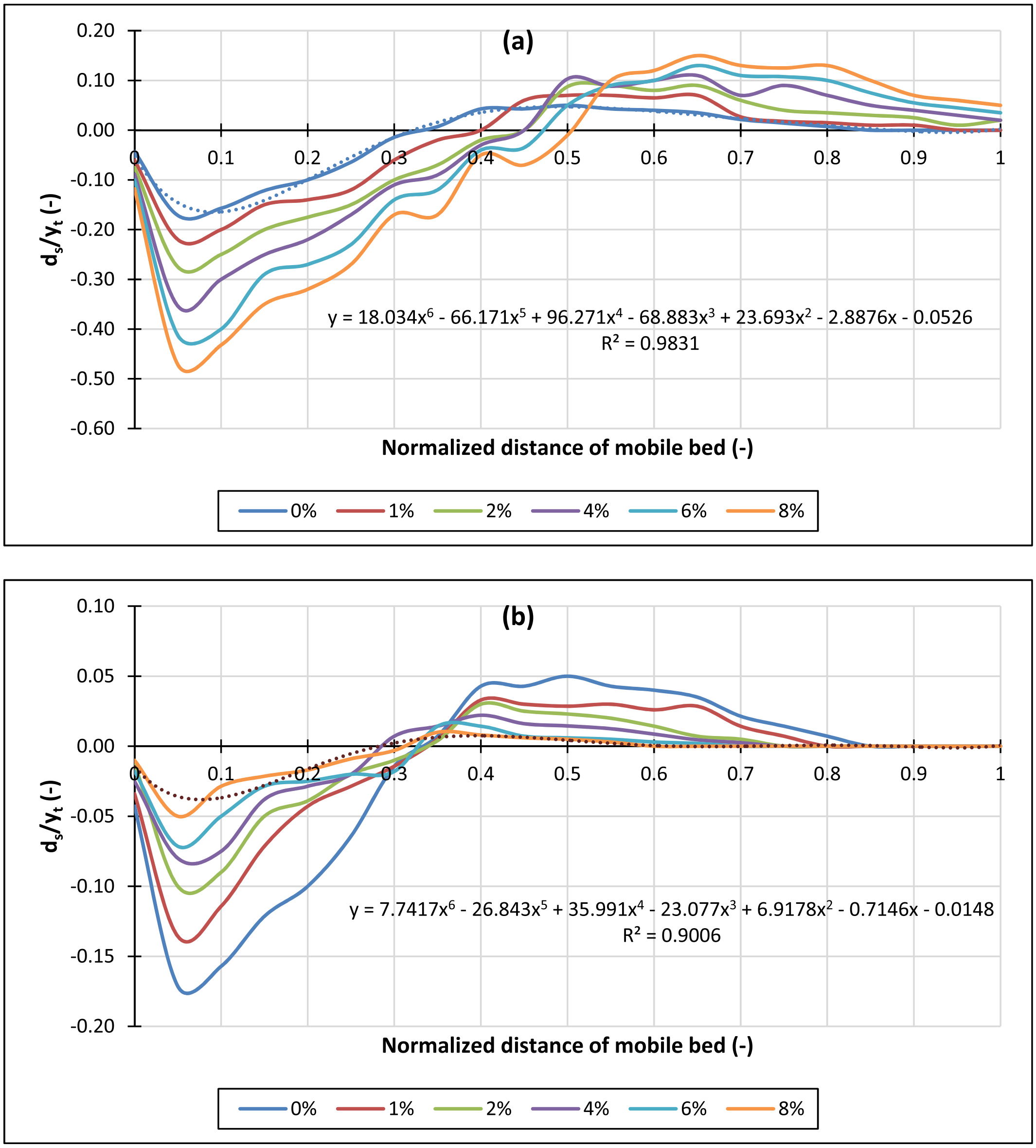

Fig. 5 The centerline bed profile for different percentages of Silica fume: (a) Dry-mix, (b) Wet-mix.

202.33%, respectively, for the mixture with 8% Silica fume compared to the case of fine sand.

Regression analyses are done for 0% Silica fume as the minimum case of scouring and silting depths are reported and an equation is obtained to depict the depths along with the bed profile. The obtained equation is presented in Fig. 5 (a).

For the case of wet-mix, 8% of Silica fume is associated with minimum disturbance in bed profile. That is reasoned by the particles Silica fume are attached to the fine sand in the presence of water to develop a mortar combination of bed material with sufficient resistance to scouring action. Where increasing the percentage of Silica fume in the mixture decreases remarkably the scour depth. Fig. 5 (b) demonstrates that the maximum scouring and silting depths decreased by 80.04% and 91.42%, respectively for the mixture with 8% Silica fume compared to the referenced case.

Regression analyses are done for the minimum case of scouring and silting depths for the case of 8% Silica fume wet-mix and an equation is obtained to depict the scouring and silting depths along with the bed profile. The obtained equation is given in Fig. 5 (b).

Emphasizing the location of maximum scouring and silting depths, they are uninfluenced by the Silica fume percentage under both types of mixing. The maximum scouring depths are located at a normalized distance of 0.05 along with the bed profile for both dry and wet mixtures. While the maximum silting depths are located at normalized distances of 0.65 and 0.50 along with the bed profile for the dry and wet mixtures, respectively. That is due to the absence of cohesive force in the bed material for the case of dry-mix, while the particles of Silica fume lose their kinetic energy gained by the flow dynamics at a longer normalized distance compared to the case of wet-mix.

Table 4 Percentage ratios of change in scouring and silting volumes.

% Silica fume	Volumes							
	Scouring Volume (m^3)		Silting Volume (m^3)		%-age Scouring Volume Change		%-age Silting Volume Change	
	Dry-mix	Wet-mix	Dry-mix	Wet-mix	Dry-mix	Wet-mix	Dry-mix	Wet-mix
0%	0.137		0.063		———		———	
1%	0.200	0.090	0.087	0.042	45.30	−34.65	37.71	−33.35
2%	0.271	0.066	0.115	0.027	97.27	−51.93	81.26	−57.83
4%	0.332	0.049	0.164	0.021	141.78	−64.17	159.54	−67.08
6%	0.419	0.044	0.195	0.010	204.43	−68.25	208.30	−83.87
8%	0.483	0.023	0.233	0.007	251.41	−83.05	268.79	−89.42

To summarize the influence of Silica fume percentage and type of mixing underscoring the volumes of scouring and silting; Table 4 is presented. The (+ve) and (-ve) signs refer to volumes increase and decrease, respectively. The table confirms the findings of Fig. 5 as the 8% Silica fume wet-mixed is recommended to minimize the bed configurations in terms of volumes of scouring and silting downstream of the sluice gate where the volumes are reduced by 83.05% and 89.42% for

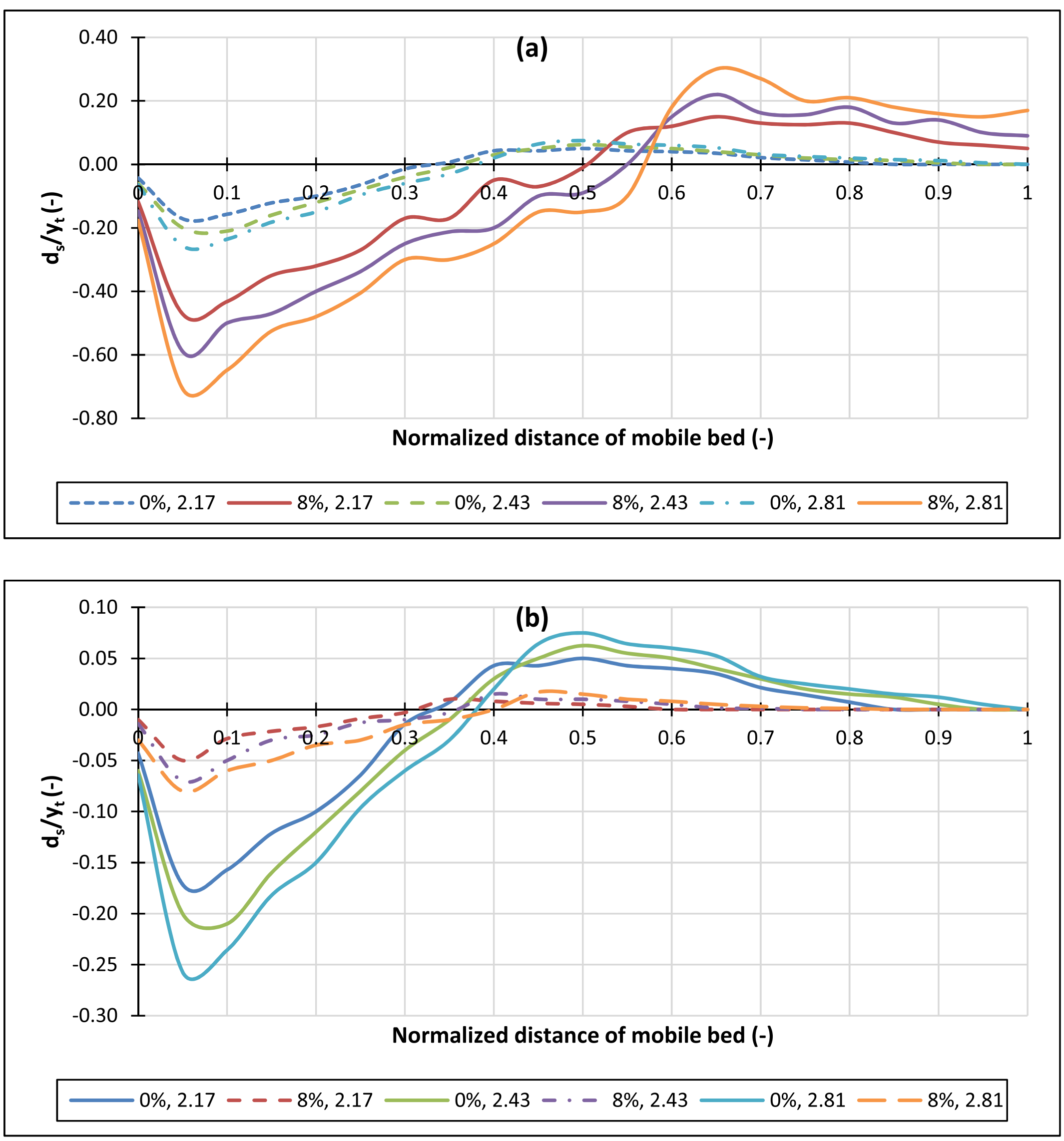

Fig. 6 The centerline bed profile for 0% and 8% Silica fume, at F_{rj} = 2.17, 2.43, and 2.81: (a) Dry-mix, (b) Wet-mix.

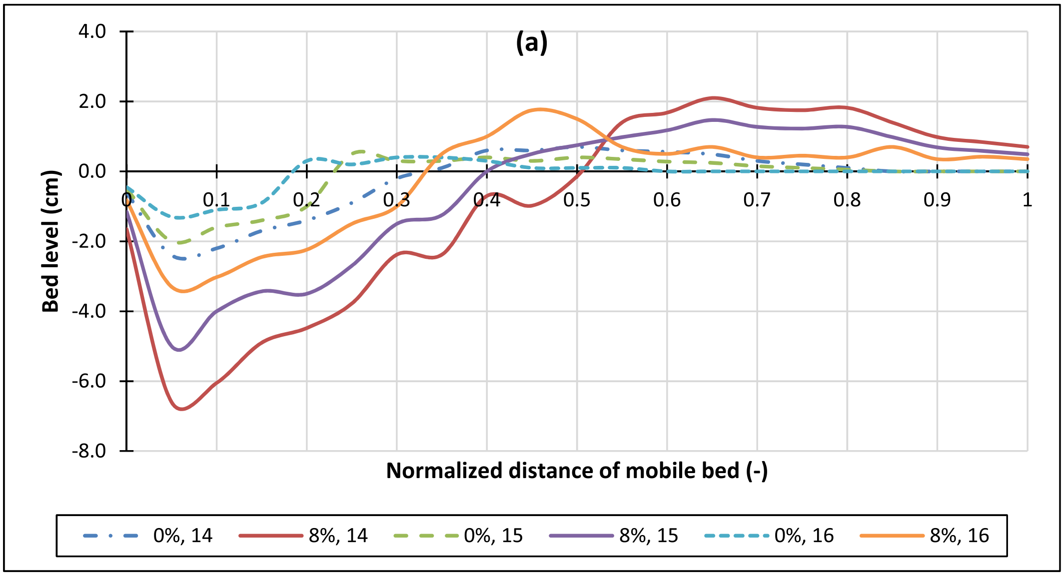

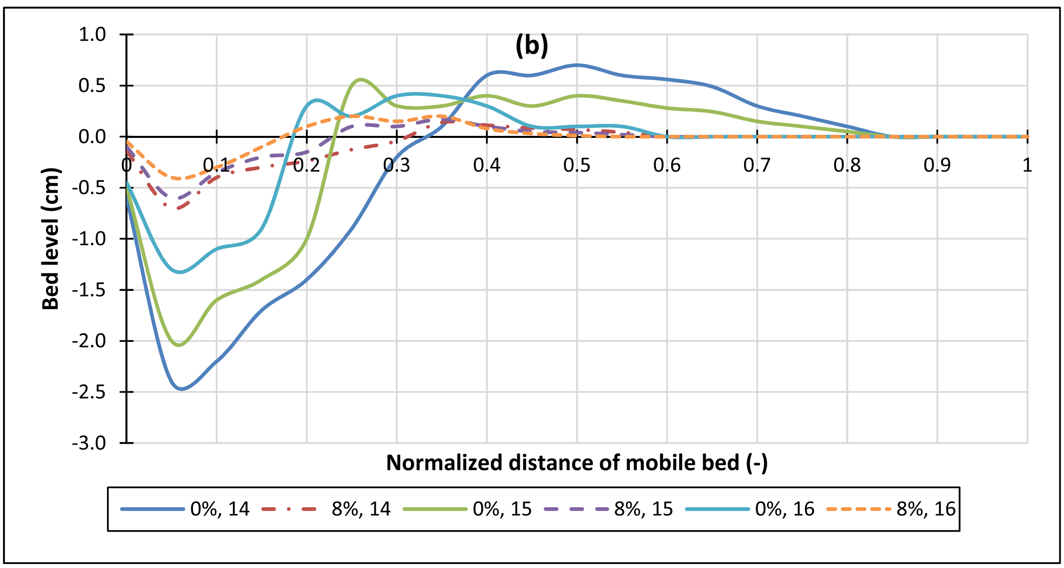

Fig. 7 The centerline bed profile for 0% and 8% Silica fume at 14, 15, and 16 cm tailwater depths: (a) Dry-mix, (b) Wet-mix.

scouring and silting, respectively. On the contrary, for the case of dry-mix, the scouring and silting volumes are increased by 251.41% and 268.79%, respectively for a similar percentage of Silica fume.

5.2. Effect of jet Froude number

Along with the bed profile, the obtained scouring and silting depths are plotted in Fig. 6 for different jet Froude numbers F_{rj} = 2.17, 2.43, and 2.81 associated to gate openings b_o = 1.00, 1.25, and 1.50 cm, respectively under constant 22 cm upstream head and 14 cm tailwater depth, (See Table 2).

The figure is plotted in the case of bed material with percentages of 0% and 8% of Silica fume for the dry and wet-mix conditions.

The figure illustrates that regardless of the Silica fume percentage and type of mixing, the bed morphological changes increase with the increase of the jet Froude number. That is because under fixed upstream and downstream water depths, whenever the gate opening increases the more discharge releases underneath the sluice gate leading to a successive increase in the jet Froude number. Therefore, the turbulences in bed material are remarkable. These findings are agreed with [9,17,24], and [37]. Based on the above results, the most critical case is associated with F_{rj} = 2.81 corresponded to b_o = 1.5 cm.

Compared to the referenced case for the bed material of 0% Silica fume, Fig. 6 (a) concerning dry-mix, the obtained results show that using 8% Silica fume prompts 175% and 300% increase in scouring and silting depths, respectively. However, under similar flow conditions and percentage of Silica fume but wet-mix, Fig. 6 (b) presents that the depths of scouring and silting decreased by 72.76% and 77.33%, respectively. Consequently, regardless of the jet Froude number, it is concluded that the wet-mix type is functional in producing a mixture of bed material with resistance to bed turbulences by the action of flow downstream of the sluice gate. These remarks are in good consistency with the conclusion in sub-section 5.1.

Underlining the location of maximum scouring depths, Fig. 6 (a) and (b) deduce that they are at a normalized distance of 0.05 along with the bed profile for both dry and wet-mix. Also, the maximum silting depths are found at normalized distances of 0.65 and 0.50 along with the bed profile for the dry and wet-mix, respectively.

5.3. Effect of tailwater depth

To explore the influence of tailwater depth on a bed material of 0% and 8% Silica fume besides the type of mixing; Fig. 7 is presented. The figure is plotted under constant 22 cm upstream water head and 1 cm gate opening to explore the bed morphology associated to flow with 14, 15, and 16 cm tailwater depths. According to Table 2, this hydraulic condition refers to jet Froude numbers of 2.17, 2.03, and 1.88. From the figure investigation, it is deduced that regardless of the presence of Silica fume and type of mixing, the geometry of scouring and silting in terms of depths and widths decrease as the tailwater depths increase. That because under constant flow discharge and cross-sectional area, both jet Froude number and flow velocity decrease as the tailwater depth increase. Therefore, this decrement in jet Froude numbers and flow velocities lead to significant limitations for the characteristics of scouring and silting where they are focal and functional parameters in the velocities.

Table 5 summarizes the maximum scouring depths for different flow conditions. The (+ve) and (-ve) signs refer to the increase and decrease in depths, respectively. The table shows that the presence of 8% Silica fume wet-mix explores relatively high performance in decreasing the bed turbulences especially for small tailwater depths. Consequently, the composition of bed material with previous specifications is assumed effective in small canals with high discharge.

5.4. Comparative study

From the previous discussion, it is concluded that using bed material with 8% Silica fume wet-mix optimally limited the bed turbulences and minimized the local scour downstream of the sluice gate under different flow conditions. To explore the effectiveness of this technique; a comparative study was implemented by considering other methodologies for controlling the local scour under similar flow conditions, therefore Fig. 8 is plotted.

Javad and Hossein [35] and Ibrahim [37] are adopted as benchmark for comparison. The advantages of using these alternatives that they applied different conventional techniques for scour protection and their measurements are reported under similar flow conditions and domains used in the current research. Javad and Hossein [35] used smooth stilling basin,

Table 5 The maximum scouring depths.

Silica fume		Maximum scour depth (cm)					
y_t (cm)	F_{rj}	Dry-mix			Wet-mix		
		0%	8%	%Change	0%	8%	%Change
14	**2.17**	2.4	6.2	158.3	2.4	0.7	−70.8
15	**2.03**	2.0	5.0	150.0	2.0	0.6	−70.0
16	**1.88**	1.3	3.2	146.2	1.3	0.4	−69.2

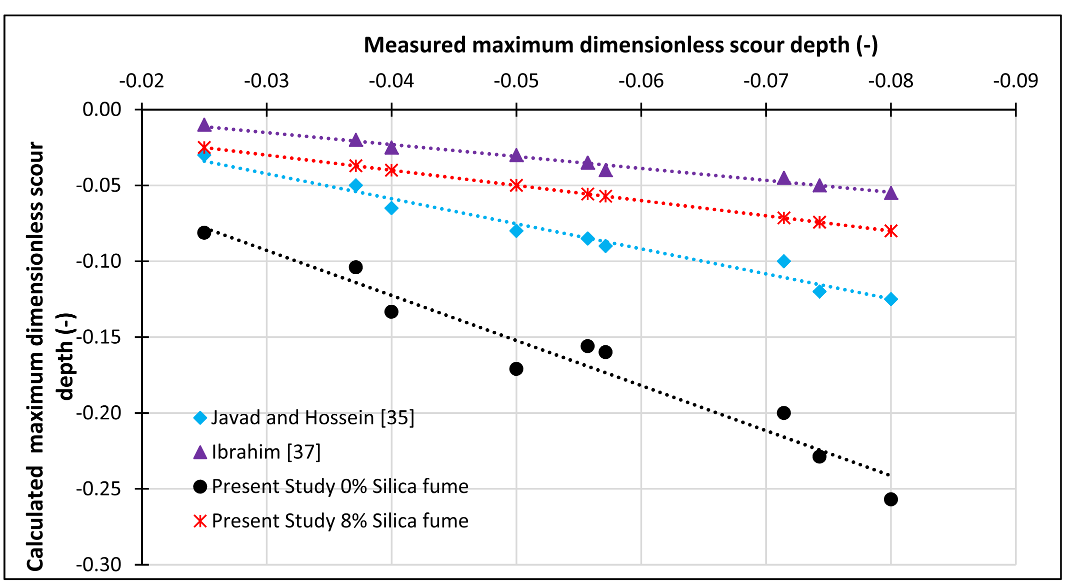

Fig. 8 Comparison between different methodologies for estimating the maximum dimensionless scour depths.

while Ibrahim [37] used an apron equipped with angled submerged vans is installed. The calculated results regarding [35] and [37] are for fine sand bed material with 0% Silica fume and without the presence of stilling basin which is the referenced case in the current study. The figure shows that the scouring depths are remarkable for the referenced case, where the maximum values are found due to the absence of any protection techniques. Using bed material with 8% Silica fume wet-mix led to a 67.09% average reduction in scouring depths compared to the bed material of fine sand with 0% Silica fume.

Emphasizing the other techniques for scour protection, the figure demonstrates that the recommended mixture of bed material gives 34.13% as an average reduction in scouring depths compared to [35]. Therefore, it is concluded that the presence of bed material mixture under the given specifications might substitute the installation of the smooth stilling basin.

Fig. 8 shows the superior of angled submerged vans presented by Ibrahim [37] to decrease the average scouring depths by 36.83% compared to the bed material with 8% Silica fume. These results are due to the effectiveness of submerged vans in dissipating the energy of hydraulic jump before the flow reaches the region of the bed material.

6. Conclusions

This research presented unconventional technique for controlling the scour downstream sluice gate. The study analyzed the effect of mixing Silica fume as a Nanomaterial to the fine sand to produce a bed material with resistance specifications to scour downstream sluice gate. The tests are carried out under limited conditions, $0\% \leq M_r \leq 8\%$; $1.88 \leq F_{rj} \leq 2.81$. Five percentages of Silica fume, 1%, 2%, 4%, 6%, and 8% were mixed to the fine sand with and without water. Based on the present experimental study, it can be concluded that the dry mixture of find sand and Silica fume regardless its percentage should not be used as bed material downstream the sluice gate because the scour is significantly increased compared to the bed material of pure fine sand. Moreover, in case of dry-mix, the bed configurations in terms of local scour and silting are directly increased with the percentage of Silica fume.

On the contrary, the case of wet-mix led to noticeable reduction in the dimensions of scouring and silting where using bed mixture of 8% Silica fume wet-mix showed 83.05% and 89.42% decrease in scouring and silting volumes, respectively compared to fine sand bed material. Also, from practical and financial aspects this mixture could replace the smooth stilling basin downstream of a sluice gate installed in small waterways. The location of maximum scouring depth is unaffected by the flow conditions and the type of bed material. The scouring and silting depths are increased as the jet Froude number increased regardless the type of mix and percentage ratio of Silica fume. The findings of this research can be applied for scour estimation downstream sluice gate of hydraulic structures.

To improve the study, it is recommended for further works to investigate wide ranges of Silica fume more than 8% under similar and different flow conditions. Also, different percentages of soft clay may be tried with Silica fume to produce a composition of Nanomaterial mixed with the fine sand as a bed material. The optimum bed composition presented in the current study may be investigated considering weirs as a heading up hydraulic structure.

Declaration of Competing Interest

The authors declare that they have no known competing financial interests or personal relationships that could have appeared to influence the work reported in this paper.

References

[1] M. Hossam, M. Mohamed, M. Ahmed, A.M. Abdel, F. Abdelhaleem, Minimizing downstream scour due to submerged hydraulic jump using corrugated aprons, Ain Shams Engineering Journal 5 (2014) 1059–1069.

[2] Lim S. and Yu G. Scouring downstream of sluice gate. Proc. First International Conference on Scour of Foundations, Texas USA, 2002; 1, pp. 395-409.

[3] Z. Tarapore, Scour below a submerged sluice gate M. Sc. Thesis, Univ. of Minnesota, USA, 1956.

[4] Y. Basmaci, Localized Scour under Vertical Gates by Submerged Jets, M. Sc. Thesis, Middle East Tech. Univ. Turkey (1971).

[5] N. Rajaratnam, Erosion by plane turbulent jets, Journal of Hydraulic Research 19 (1981) 339–358.

[6] K. Ali, S. Lim, Local scour caused by submerged wall jets, Proc. ICE Part 2; 81 (1986) 607–645.

[7] Valentin F. Considerations concerning scour in the case of flow under gates. Proc. 12th Cong. IAHR, 1967; 3, pp. 92-96.chen

[8] Altinbilek H. and Basmaci Y. Localized scour at the downstream of outlet structures, in Proceedings of the 11th Congress on Large Dams. Madrid, 1973, pp. 105–121.

[9] Breusers H. and Raudkivi A. Scouring. IAHR Hydraulic Structures Design Manual, AA Balkema, 1991.

[10] S. Chatterjee, S. Ghosh, M. Chatterjee, Local scour due to submerged horizontal jet, Journal of Hydraulic Engineering 120 (8) (1994) 973–992.

[11] O. Aderibigbe, N. Rajaratnam, Effect of sediment gradation on erosion by plane turbulent wall jets, Journal of Hydraulic Engineering 124 (10) (1998) 1034–1042.

[12] B. Melville, S. Lim, Scour caused by 2D horizontal jets, Journal of Hydraulic Engineering 140 (2) (2013) 149–155.

[13] S. Gamal, Estimation of the min floor length behind sluice gates against scour utilizing solid bed and erodible basin, Journal of Engineering Sciences, Assiut University 34 (4) (2006) 1159–1174.

[14] Melville B. Scour at Various Hydraulic Structures: Sluice gates, Submerged bridges, Low weirs. 5th International Symposium on Hydraulic Structures Brisbane, Australia, 2014; pp. 25-27.

[15] X. Chen, Y. Siow, Effects of Jet Flipping on Local Scour Downstream of a Sluice Gate, Journal of Hydraulic Engineering 141 (4) (2015).

[16] M. Najafzadeh, Neuro-fuzzy GMDH based particle swarm optimization for prediction of scour depth at downstream of grade control structures, Eng. Sci. Technol. Int. J. 18 (2015) 42–51.

[17] M. Najafzadeh, A. Tafarojnoruz, S.Y. Lim, Prediction of local scour depth downstream of sluice gates using data-driven models, ISH J. Hydraul. Eng. 23 (2017) 195–202.

[18] A. Yousif, O. Sadeq, D. Lamine, E. Mohammad, S. Shamsuddin, N. Al-Ansari, M. Zaher, Open Channel Sluice Gate Scouring Parameters Prediction: Different Scenarios of Dimensional and Non-Dimensional Input Parameters. Journal of, Water 11 (2019) 353.

[19] S. Ahmad, T. Ali, S. Mojtaba, M. Zaher, Simulation of the depth scouring downstream sluice gate: The validation of newly developed data-intelligent models, Journal of Hydro-environment Research 29 (2020) 20–30.

[20] C. Mehmet, K. Cimen, Numerical simulation of scour at downstream of submerged sluice flow, Pamukkale University Journal of Engineering Sciences 24 (3) (2018) 439–443.

[21] B. Hamid, S. Erfaneh, P. Vijay, Prediction of Local Scour Depth Downstream of Sluice Gates Using Harmony Search Algorithm and Artificial Neural Networks, Journal of Irrigation and Drainage Engineering 144 (5) (2018).

[22] S. Hamidreza, K. Amir, R. Masoumeh, M. Mojtaba, C. Yovanni, Numerical simulation of scour and flow field over movable bed induced by a submerged wall jet, Journal of Hydroinformatics 22 (10) (2020).

[23] A. Chaudhary, Studies on Scour due to Submerged Horizontal Jet M.Tech Thesis, Kurukshetra University, Kurukshetra, 1995.

[24] M. Verma, G. Arun, Scour downstream of a sluice gate, ISH Journal of Hydraulic Engineering 11 (3) (2005) 57–65.

[25] Iwagaki Y., Tsuchiya Y., and Imamura M. Studies of the Local Scour from Flows Downstream of an Outlet (1). Disaster Prevention Research Institute, Annuals No. 8, Kyoto University, Japan, 1965, pp. 363-377.

[26] N. Hassan, R. Narayanan, Local Scour Downstream of an Apron, J. Hydr. Engrg, ASCE 111 (11) (1985) 1371–1385.

[27] Li W. Scour of Fine Sediment by a Turbulent Wall Jet. Ph.D. Thesis, Lamar University, Texas, USA; 1993.

[28] Lim Siow-Yong and Yu Guoliang. Scouring Downstream of Sluice Gate. First International Conference on Scour of Foundations, ICSF-1, Texas A&M University, College Station, Texas, USA, November 17-20, 2002.

[29] C. Luis, C. Elsa, A. Rui, M. Maria, Experimental study of the bed morphology downstream of a sluice gate, 9th Conference on Fluvial Hydraulics, River Flow, 2018.

[30] M. Ibrahim, Improve the efficiency of stilling basin using different types of blocks, American Journal of Engineering Research 6 (8) (2017) 295–304.

[31] H. Alireza, Experimental Study of Submerged Hydraulic Jumps with Baffle Blocks Ph.D. Thesis, University of Alberta, Canada, 2013.

[32] M. Valinia, S. Ayyoubzadeh, M. Yasi, Effect of Baffle blocks on the geometry of scour hole downstream of stilling basins, Iranian Water Research Journal 2 (33) (2019) 11–19.

[33] Saleh O., Negm A., Waheed-Eldin, and Noha G. Effect of End Sill on Scour Characteristics Downstream of Sudden Expanding Stilling Basins. Eighth International Water Technology Conference, IWTC8 2004, Alexandria, Egypt.

[34] Ohsen N., Mohamad H., and Hossein H. Local scouring at bed sill downstream of turbulent jets. E-proceedings of the 36th IAHR World Congress, 28 June – 3 July 2015, The Hague, the Netherlands.

[35] F. Javad, K. Hossein, Investigation on local scour downstream of adverse stilling basins, Ain Shams Engineering Journal 5 (2014) 361–375.

[36] K. Yehia, S. Shazy, O. Aya, Energy dissipation downstream sluice gate using a pendulum sill, Alexandria Engineering Journal 57 (2018) 3977–3983.

[37] M. Ibrahim, Effect of angled submerged vanes on bed morphology downstream sluice gate, Journal of Scientific Research & Reports 22 (4) (2019) 1–16.

[38] R. Akbar, Numerical investigation of the effect of air injection on the flow parameters and feasibility of scour reduction downstream of the stilling basin MSc Thesis, Tarbiat Modares University, Iran, 2018.

[39] Hanifeh Imanian, Abdolmajid Mohammadian, Numerical simulation of flow over ogee crested spillways under high hydraulic head ratio, Engineering Applications of Computational Fluid Mechanics 13 (1) (2019) 983–1000, https://doi.org/10.1080/19942060.2019.1661014.

[40] James Yang, Penghua Teng, Hongwei Zhang, Experiments and CFD modeling of high-velocity two-phase flows in a large chute aerator facility, Engineering Applications of Computational Fluid Mechanics 13 (1) (2019) 48–66, https://doi.org/10.1080/19942060.2018.1552201.

[41] Mehrshad Samadi, Ebrahim Jabbari, H.M. Azamathulla, Mohammad Mojallal, Estimation of scour depth below free overfall spillways using multivariate adaptive regression splines and artificial neural networks, Engineering Applications of Computational Fluid Mechanics 9 (1) (2019) 291–300, https://doi.org/10.1080/19942060.2015.1011826.

[42] Sammen, S.Sh., Mohammad Ali Ghorbani, Anurag Malik, Yazid Tikhamarine, Mohammad Amir Rahmani, Nadhir Al-Ansari, and Kwok-Wing Chauet. Enhanced Artificial Neural Network with Harris Hawks Optimization for Predicting Scour Depth at Downstream of Ski-Jump Spillway. Appl. Sci. 2020, 10, 5160; doi:10.3390/app10155160

[43] M. Ted, R. Rachael, R. Santosh, D. Brian, A. Juan, D. Larry, Scour Reduction by Air Injection Downstream of Stilling Basins: Optimal Configuration Determination by Experimentation, J. Irrig. Drain Eng. Vol. 142(12) (2016).

[44] E. Gamal, M. Abdelazim, A.N. El-Hazek, M. Ahmed, Influence of Using Floor Jets on the Local Scour Downstream Fayoum Type Weir, Asian Journal of Engineering and Technology 8 (1) (2020) 13–22.

[45] Khalifehei K., Azizyan G., Shafai-Bajestan M., and Chau K. W. Experimental Modeling and Evaluation Sediment Scouring in Riverbeds around Downstream in Flip Buckets. International Journal of Engineering (IJE), IJE TRANSACTIONS A: 2020; Basics Vol. 33, No. 10, pp.1904-1916.

[46] K. Khalifehei, G. Azizyan, M. Shafai-Bajestan, K.W. Chau, Stability of A-Jack Concrete Block Armors Protecting the Riverbeds, Ain Shams Engineering Journal 12 (2021) 381–391.

[47] G. Amir, D. Rasoul, Z. Reza, A. Forough, Experimental investigation of downstream erosion control of stepped spillways using MicroSilica- structured and Nanomaterials. Amirkabir, Journal of Civil Engineering (2019).